The Effects of Regional Pulmonary Blood Flow on Protein Flux Measurements with PET

Aaron Hamvas, James D. Kaplan, Joanne Markham, and Daniel P. Schuster

From the Departments of Pediatrics, the Biomedical Computer Laboratory, and Internal Medicine, Washington University School of Medicine, St. Louis, Missouri

We used PET to evaluate whether changes in regional pulmonary blood flow (PBF) or plasma volume (PV) affect calculations of the pulmonary transcapillary escape rate (PTCER) for ^{68}Ga-labeled transferrin. We reduced PBF in five dogs by inflating a right atrial balloon. Regional PBF decreased 25% to 174 ± 40 ml/min/100 ml lung without a change in PV or PTCER. In eight other dogs, we decreased PBF and PV via controlled arterial hemorrhage. PBF decreased 45% to 110 ± 33 ml/min/100 ml lung and PV decreased 22% without a change in PTCER. We also used a series of computer simulations to evaluate the effect of even greater reductions in regional PBF on PTCER calculations. These simulations showed, in support of the experimental data, that if PBF was >40 ml/min/100 ml lung, PTCER could be accurately measured. However, below this level, PV was increasingly underestimated and PTCER overestimated. The results indicate the sensitivity of the PTCER calculation to errors in the PV measurement, especially in regions of markedly reduced regional PBF.

J Nucl Med 1992; 33:1661–1668

T he most common paradigm for pulmonary edema divides potential etiologies into two general categories: cardiogenic and noncardiogenic. Noncardiogenic pulmonary edema (NCPE) is presumed to result from increased pulmonary vascular permeability to water and protein. Clinically, however, the diagnosis of NCPE depends on inference because no noninvasive method has been generally accepted as accurate.

External radiation detection methods are perhaps the most commonly used technique to clinically evaluate pulmonary vascular permeability. With these methods, a radioactively labeled protein tracer is administered intravenously, and its accumulation in lung tissue, relative to its blood concentration, is followed over time. The time-activity data in both lung tissue and blood are then interpreted mathematically, usually with some variation of a two-compartment (vascular and extravascular) model (1–

4). Both Roselli et al. (5) and Mintun et al. (6) have recently shown that these methods share a common mathematical foundation and set of assumptions. However, since the final mathematical expression is ultimately a measure of the permeability-surface area product for the protein, these calculations should also be sensitive to changes in membrane exchange surface, as well as to any real change in the rate of protein flux per unit surface area. Thus, many investigators divide the permeability-surface area product expression by a measure of regional pulmonary plasma volume (1–4,6), assuming, of course, that changes in pulmonary plasma volume directly reflect changes in surface area.

The two-compartment model also assumes that the vascular tracer concentration is independent of blood flow through the vascular compartment (i.e., tracer turnover is high). This is certainly true under normal conditions, but many pulmonary edema states are characterized by profound regional decreases in pulmonary blood flow, and under such circumstances this assumption might not be valid.

In previous studies (4,7,8), we used positron emission tomography (PET) to evaluate pulmonary vascular permeability by measuring the pulmonary transcapillary escape rate (PTCER) for ^{68}Ga-labeled transferrin. Since PET can also be used to independently measure plasma volume and blood flow in the same regions evaluated for changes in permeability, we designed the following set of experiments and computer simulations to see if PTCER calculations were significantly affected by changes in either regional pulmonary blood flow or plasma volume.

METHODS

Animal Preparation

Eighteen mongrel dogs weighing 20–25 kg were anesthetized with intravenous pentobarbital (30 mg/kg), intubated with a cuffed endotracheal tube and ventilated with an inspired oxygen fraction of 1.0 using a Harvard animal ventilator. Tidal volume and ventilatory rate were adjusted to keep PCO_2 approximately 35–45 mmHg. Additional barbiturate was administered as necessary to maintain a surgical plane of anesthesia. Through bilateral femoral incisions, a balloon tipped pulmonary arterial catheter and a 100 cm 7.0-Fr pig-tailed catheter were positioned fluoroscopically in the pulmonary artery. A catheter was placed in the femoral artery for blood sampling, and a 5-cm 20-gauge

catheter was placed in the jugular vein for radiopharmaceutical administration. In 10 dogs, a 16 Fr Foley catheter with a 30-ml balloon was inserted under fluoroscopic control via the right jugular vein into the right atrium.

Cardiac output was measured in triplicate by the thermodilution technique using an Edwards Laboratories cardiac output computer. Transducers were calibrated to the center of the lateral chest and connected to a Mennen Model 742 monitor for pulmonary arterial, pulmonary capillary wedge and systemic arterial pressures. Blood gases were analyzed using an Instrumentation Laboratories Model 813 blood gas analyzer.

Experimental Protocols

The experimental protocols included blank and transmission PET scans (used to correct for photon attenuation during the emission scans and to place regions of interest (ROIs) for image analysis), a baseline "data set," a manipulation to decrease cardiac output and/or blood volume, and finally, another "data set." For these studies, a data set included: (1) a 15-sec scan during a continuous infusion of 2.2 × 10^9–2.9 × 10.9 Bq^{15}O-water (used for the PBF measurement), (2) a 300-sec scan after equilibration of the ^{15}O-water (to measure the apparent blood-tissue partition coefficient needed for the PBF calculation) (7), (3) a 45-min scan after injecting ^{68}Ga-citrate (used to measure PTCER), and (4) pulmonary arterial, pulmonary capillary wedge, and mean systemic arterial pressures, and cardiac output.

After the baseline data set was completed, the ^{68}Ga ($t_{1/2}$ = 68 min) was allowed to decay for approximately 3 hr. During the latter half of this period, the cardiac output was decreased by either of two means (see below), and the animal was allowed to stabilize for an additional 30 min. The second data set was then obtained. For the baseline PTCER measurements, 7.4–11.1 × 10^7 Bq of ^{68}Ga-citrate were injected, while 30–37 × 10^7 Bq ^{68}Ga were injected for the second PTCER measurement. Background counts in lung tissue and blood at the beginning of the second data set were approximately 5% of those obtained following the second ^{68}Ga injection. This background activity was subtracted from the second set of measurements, with appropriate corrections for further radioactive decay during the second 45-min scan.

In five dogs (RA balloon group), cardiac output was reduced by inflating the right atrial Foley catheter balloon until cardiac output decreased approximately 40%. In eight other dogs (Hemorrhage group), 600–700 ml of arterial blood were removed until cardiac output also decreased approximately 40%. Finally, in the remaining five animals (Control group), although instrumented like the RA balloon group, we performed no intervention to reduce cardiac output between data sets.

PET Techniques

All PET measurements were performed with the PETT VI system. Design features, methods for calibration, corrections for activity decay and corrections for photon attenuation have been discussed elsewhere (9). The animal was placed in the scanner in the supine position with the most caudal transaxial PET slice at the level of the dome of the diaphragm.

Pulmonary Blood Flow Measurements. Our methods for measuring PBF with PET have been described previously in detail (10). Two periods of radioactivity data collection are required after administering H$_2$^{15}O. First, a 15-sec scan is performed during a 20-sec constant infusion of ^{15}O-water, while blood is withdrawn simultaneously from the pulmonary artery. This scan measures the initial distribution of the water tracer in the pulmonary

circulation. Then, after a 4-min equilibration period, a 300-sec data collection is begun, again with simultaneous peripheral arterial blood sampling. Data from this scan are used to determine the apparent regional partition coefficient for the tracer since PET data are expressed in units of lung volume and regional inflation is variable within the lung. During both phases, the blood activity is measured in a calibrated well counter. These blood time-activity and tissue time-activity data are interpreted with a one-compartment mathematical model to yield the PBF images. PBF measurements with this technique correlate closely with measurements using ^{68}Ga-labeled microspheres (10,11). Regional PBF is expressed as ml/min/100 ml lung.
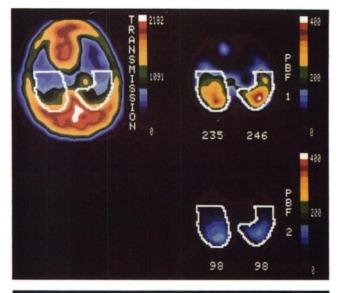
Plasma Volume Measurement. Gallium-68-citrate is prepared according to previously described methods (12) and injected intravenously. The citrate rapidly dissociates and the ^{68}Ga binds avidly to transferrin, a serum protein with a molecular weight and permeability properties similar to those of albumin (13). Two minutes after injection, a 90-sec PET scan is performed while peripheral blood samples are obtained simultaneously. Regional plasma volume (PV) is calculated from the ratio of the tissue time-activity data (Q(t)) to that in blood (Bl(t)) during the same 90-sec scan period (i.e., PV = Q(t) (1-Hct)/Bl(t), where Hct = hematocrit). Regional plasma volume is expressed as ml/100 ml lung.

PTCER Measurement. PTCER is also measured after the same ^{68}Ga-citrate injection. Fourteen 90-sec and five 300-sec scans are obtained over a 45-min period, beginning 2 min after tracer injection. Simultaneously, blood activity is measured by periodic sampling of arterial blood during the scans. Time-activity curves are created for the circulating blood activity and for PET tissue activity in the ROI and are decay-corrected to the time of injection. Marquardt-Levenberg parameter estimation techniques are then used to calculate a forward (k_1) and reverse (k_2) rate constant from the time-activity data in a two-compartment (vascular and extravascular) model (see Appendix). PTCER is calculated as k_1/PV and is expressed as 10^{-4} min^{-1}.

Data Analysis. For this study, ROIs were defined in the dorsal half of each transverse tomographic transmission image. The regions were bounded by the dorsal aspect of the heart (the left atrial level), the chest wall and the midline of the image (Fig. 1). The regions were limited to the dorsal half of the image to avoid potential partial volume averaging effects from the heart. The regions were kept in computer memory so that identical regions could be serially evaluated with each successive scan. A minimum of four regions from two to three slices were analyzed for each dog. Measurements were averaged for each dog and then for the experimental group as a whole.

Data are presented as means ± 1 s.d. Analysis of variance techniques were used to compare mean values among the various experimental groups using the Statistical Analysis System (SAS, Cary, NC) for the IBM-PC computer. Statistical significance was accepted for p < 0.05.

Computer Simulations. Although the two experimental protocols used in this study resulted in a 40%–50% reduction in regional PBF, further reductions were not possible in a hemodynamically stable and viable animal preparation. Therefore, to evaluate the effect of even greater reductions in regional PBF on the PTCER calculation, we performed the following computer simulations and analyses. All simulations were performed with programs written in FORTRAN and executed with a Concurrent Model 3205 computer.
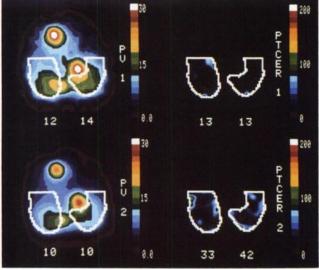
FIGURE 1. ROIs are indicated on representative PET images from one dog in the Hemorrhage group. The dog is supine, and the left side of the animal is on the left side of the image. (Top) Transmission scan (units on the color scale are in arbitrary "PETT numbers") and the PBF images and values before and after hemorrhage (PBF 1 and PBF 2, respectively). (Bottom) Plasma volume (PV1 and PV2) and PTCER (PTCER 1 and PTCER 2) images and values before and after hemorrhage. PBF = pulmonary blood flow (ml/min/100 ml lung), PV = plasma volume (ml/100 ml lung) and PTCER = pulmonary transcapillary escape rate (10^{-4} min^{-1}).

First, we modified the two-compartment model just referred to above (now designated as MODEL-NOPBF) to include regional PBF as a parameter (now designated as MODEL-PBF). The derivation of the relevant model equations is presented in the Appendix. With the use of MODEL-PBF, we generated a group of tissue time-activity curves to simulate the activity data that might be obtained during the study of an animal with either a normal PTCER or an abnormally high PTCER over a wide range of PBF. To produce the simulated data curves, values for vascular volume and for both PTCER and the reverse transport rate constant (k_2) were assigned to a hypothetical lung region. The values chosen were typical of both conditions, as measured

in previous studies (6). Thus, a family of tissue time-activity curves was created for both the normal and high permeability conditions, each curve representing the expected tissue time-activity data at a different regional PBF.

The blood time-activity relationship was assumed to be the same for both conditions, and was described by a simple biexponential equation of the form:

$$Bl(t) = Ae^{-\alpha t} + Be^{-\beta t}, \qquad \text{Eq. 1}$$

where $Bl(t)$ is the concentration of activity in blood as function of time (t) and the values for parameters α, β, A and B were obtained by nonlinear optimization. This equation was found empirically to accurately describe the blood time-activity data between 2 and 60 min after intravenous protein tracer injection, as obtained in previous experiments (4).

After generating the tissue time-activity data for the various values of PBF, we then re-calculated PTCER from these data using MODEL-NOPBF, i.e., the model originally reported (4), which assumes that tracer concentration is independent of regional PBF. The PTCER used to generate the tissue time-activity curves from MODEL-PBF is referred to as "PTCER-true," while PTCER *calculated* from these data with MODEL-NOPBF is referred to as "PTCER-observed." The differences between PTCER-true and PTCER-observed were expressed as a percent error.

RESULTS

RA Balloon Group

After inflation of the atrial balloon, cardiac output decreased 40% ± 6%. There was no change in the other hemodynamic parameters (Table 1). With the reduction in cardiac output, measured PBF decreased 25% on average in the regions analyzed. Neither regional plasma volume nor k_1 changed significantly. Therefore, PTCER was also unchanged (Table 2).

Hemorrhage Group

In this group, 586 ± 102 ml blood were removed, resulting in a 46% ± 6% reduction in cardiac output. The mean systemic blood pressure, mean pulmonary artery pressure and pulmonary capillary wedge pressure also decreased significantly (Table 1). Hematocrit increased 1 hr after hemorrhage. Regional PBF decreased an average of 49% (p < 0.05) and regional PV decreased 22% (p < 0.05) after hemorrhage. Estimated values for k_1 decreased 31% on average (Table 2) but were not statistically significant because k_1 increased in four dogs and decreased in the other four (Fig. 2). There was no statistically significant relationship between the reduction in PV and the change in k_1 (r = 0.36). However, PTCER for this group remained within the normal range (see "normal PTCER values" below) following PBF and PV reduction. Representative PET images from one dog before and after hemorrhage are displayed in Figure 1 and demonstrate a reduction in regional PBF and PV without a change in PTCER.

Control Group

There was no significant difference in any of the hemodynamic or PET-derived measurements between Time 1 and Time 2 in the Control group (Tables 1 and 2).

TABLE 1
Hemodynamic Measurements

Protocol	CO (liter/ min)	BP (mmHg)	PA (mmHg)	WP (mmHg)	Hct
RA balloon (n = 5)					
Time 1	3.1 ± 0.3	128 ± 12	8 ± 3	3 ± 2	0.40 ± 0.03
Time 2	1.9 ± 0.1*	115 ± 10	9 ± 2	4 ± 7	0.40 ± 0.03
Hemorrhage (n = 5)					
Time 1	2.5 ± 0.1	130 ± 7	10 ± 5	5 ± 4	0.42 ± 0.04
Time 2	1.4 ± 0.2*	96 ± 19*	7 ± 5*	3 ± 3*	0.45 ± 0.03*
Control (n = 5)					
Time 1	2.7 ± 0.5	138 ± 21	14 ± 4	4 ± 2	0.41 ± 0.05
Time 2	2.5 ± 0.4	138 ± 25	14 ± 4	6 ± 2	0.41 ± 0.05

* $p < 0.05$ compared with Time 1.

Time 1 = baseline; Time 2 = after CO manipulation; CO = cardiac output; BP = mean systemic arterial pressure; PA = mean pulmonary arterial pressure; WP = pulmonary capillary wedge pressure; and Hct = hematocrit.

Data are expressed as mean ± s.d.

Normal PTCER Values

Previously, we used data from four dogs to establish "normal" values for PTCER in dogs. To expand this data base further, PTCER measurements from the Control group at both time points were averaged with the baseline values from the RA balloon and Hemorrhage groups. PTCER averaged $44 \pm 31 \, 10^{-4}/min^{-1}$, which is not significantly different from the previously reported values of $49 \pm 18 \, 10^{-4}/min^{-1}$ (10).

Computer Simulations

The specific values used to generate a family of tissue time-activity curves for various values of PBF by computer simulation as well as for a blood time-activity curve are given in Table 3. The derived tissue time-activity curves for each condition (normal and high permeability) are shown in Figure 3 along with the curve representing blood activity within the hypothetical ROI (i.e., blood activity multiplied by blood volume). The simulated data show

that with decreasing regional PBF, the time to peak tissue activity is progressively lengthened. The slow rise in activity for low flow reflects the vascular mean transit time ($\bar{t}$ = BV/PBF), which for a flow of 20 ml/min/100 ml lung and a blood volume of 20 ml/100 ml lung is about 1 min.

Figure 4 shows the effect of using MODEL-NOPBF to calculate PTCER, assuming the tissue and blood time-activity curves shown in Figure 3. PTCER would be accurately calculated for both low and high permeability conditions if PBF was >40 ml/min/100 ml lung. For PBF less than 40, PV would be progressively underestimated, resulting in overestimation of both k_1 and PTCER (by as much as several hundred percent). Indeed, for the normal condition, PTCER would become sufficiently high to be confused with truly abnormal values (Fig. 4D).

DISCUSSION

When using PET to evaluate pulmonary vascular permeability by measuring the rate of protein flux between

TABLE 2
PET Measurements

Protocol	PBF (ml/min/100 ml lung)	k_1 (10^{-4} ml/min/100 ml lung)	PV (ml/100 ml lung)	PTCER (10^{-4} min^{-1})
RA balloon (n = 5)				
Time 1	233 ± 32	544 ± 434	12.6 ± 0.6	44 ± 34
Time 2	174 ± 40*	786 ± 457	12.9 ± 1.8	59 ± 27
Hemorrhage (n = 8)				
Time 1	217 ± 38	644 ± 626	13.9 ± 1.3	48 ± 46
Time 2	110 ± 33*	447 ± 248	10.8 ± 0.7*	40 ± 23
Control (n = 5)				
Time 1	225 ± 43	530 ± 193	12.1 ± 1.7	45 ± 18
Time 2	186 ± 17	428 ± 170	11.4 ± 1.3	37 ± 13

Data are expressed as mean ± s.d. PBF = pulmonary blood flow, PV = regional blood volume and PTCER = pulmonary transcapillary escape rate.
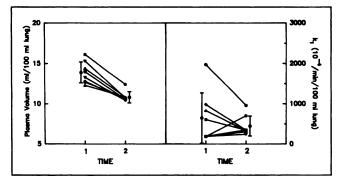
* $p < 0.05$ compared to Time 1 in the same protocol.

FIGURE 2. The PET-measured changes in regional plasma volume and k_1 at each time for the individual dogs in the Hemorrhage group. Each symbol represents one dog; the filled circles and error bars represent the mean values ± 1 s.d.

vascular and extravascular compartments, we have made the following assumptions:

1. All tracer activity is intravascular for the first 3 min after intravenous injection.
2. Movement of tracer across the pulmonary capillary endothelium is passive.
3. The concentration of tracer in peripherally sampled blood is equivalent to that in pulmonary vascular blood.
4. Regional pulmonary PV does not change during the course of the scan.
5. Tracer concentration in the vascular compartment is independent of tracer delivery to the intravascular compartment.
6. Plasma volume varies linearly with vascular surface area and therefore is an appropriate index to normalize k_1.

In the current study, we provide evidence concerning the validity of assumptions 5 and 6. The results demonstrate the sensitivity of the PTCER calculation to errors in the PV measurements, especially in regions of markedly reduced PBF. Furthermore, changes in k_1 correlate poorly

TABLE 3
Model PBF Parameters

	Norm-True	High Perm-True
PTCER	45	750
k_1	540	9,000
k_2	198	11,700
PV	12	12

Values for the parameters used in the computer simulations for normal (Norm-True) or high permeability (High Perm-True) conditions. The blood curve defined by Equation 1 is the same for both the normal and high permeability conditions. The coefficients are A = 8317, B = 7500, $\alpha = 1.38 \times 10^{-4}$, $\beta = 21.4 \times 10^{-4}$. Units used are: PTCER 10^{-4} min^{-1}, PV ml/100 ml lung, k_1 and k_2 10^{-4} ml/min/100 ml lung.
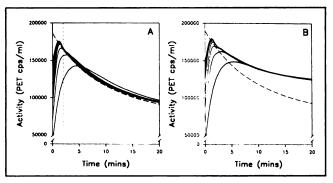
FIGURE 3. Simulated time-activity curves for normal (A) and high permeability (B) conditions, as generated by MODEL-PBF using the parameter values listed in Table 3. The solid lines represent the tissue time-activity curves for discrete values of PBF between 10 and 100 ml/min/100 ml lung in increments of 10 ml/min/100 ml lung. The dashed line represents the biexponential expression for the blood time-activity curve, also using the parameter values given in Table 3. As the simulations show, the time to peak activity lengthens as PBF decreases. The vertical dotted line represents time at 2 min, the beginning of the PV measurement. Thus, at low values for PBF, as represented by the two most rightward solid curves in each panel (10–20 ml/min/100 ml lung), "tissue" activity is less than the actual input blood activity, and therefore PV will be underestimated.

with changes in PV, suggesting that PV may not be the most appropriate means of normalizing PTCER for regional differences in pulmonary vascular surface area.
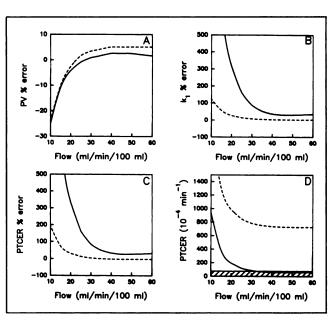
Impact of PBF on PV. Regional pulmonary PV is

FIGURE 4. Error in calculating k_1, PV and PTCER as a function of PBF, when using MODEL-NOPBF for calculations, based on the tissue and blood time-activity data shown in Figure 3, for the normal (solid lines) and high-permeability (dashed line) conditions. As PBF decreases below 40 ml/min/100 ml lung, PV is increasingly underestimated (A), resulting in an increasing overestimation (by as much as several hundred percent) in k_1 (B). PTCER is thus increasingly overestimated (C) such that calculated values for normal permeability increase outside of the normal range (D, cross-hatched area).

estimated from the 90-sec PET scan that begins 2 min after tracer injection. The equation

$$PV = Q(t)(1\text{-}Hct)/Bl(t) \qquad Eq. 2$$

describes the relationship where PV is the plasma volume, $Q(t)$ is the integrated PET activity from 2 to 3 min and $Bl(t)$ is the integrated blood activity from 2 to 3 min. Implicit in this calculation is the assumption that at the beginning of the scan all tracer activity in the image is in the intravascular compartment and is equal to the arterial tracer activity (i.e., no activity has moved to the extravascular compartment). Figure 3 shows that for PBF values greater than 30 ml/min/100 ml lung, this assumption is reasonable. However, with PBF values less than 30, equilibrium (i.e., tracer concentration in the vascular compartment equals the concentration in arterial blood) does not occur until after 2 min, resulting in an underestimation of PV.

Plasma (blood) volume did not change in those animals subjected to isovolemic blood flow reduction (RA balloon group), but did decrease significantly following hemorrhage (Hemorrhage group) (Table 2). In the Hemorrhage group, after removing approximately 30% of the calculated circulating blood volume, the PET-measured regional pulmonary PV decreased 22%. This change was comparable to the 20% decrease measured after a similar degree of blood removal in an earlier study (14). Neither blood flow reduction technique decreased regional PBF to the point that measurement errors in PV would be likely, as predicted from Figures 3 and 4.

While cardiac output was decreased to a similar amount in the two experimental groups, regional PBF decreased to a greater extent in the Hemorrhage group. With the decrease in blood volume, pulmonary capillaries may have been de-recruited, thereby increasing pulmonary vascular resistance, while pulmonary perfusion pressures also decreased, resulting in disproportionate decreases in PBF (Tables 1 and 2). In contrast, neither blood volume nor perfusion pressures decreased in the RA balloon group.

Impact of PV on k_1. The data in this study show that an accurate PV measurement is essential to accurately measure k_1 (and thus, PTCER). Tissue activity is assumed to be the sum of vascular and extravascular activity,

$$Q(t) = (PV \cdot Bl(t)) + q_2(t), \qquad Eq. 3$$

where $q_2(t)$ is extravascular activity and $Q(t)$ (in contrast to Equation 2, in which $q_2(t)$ is assumed to be 0) is total tissue activity during each of the 19 separate PET images obtained for the PTCER calculation.

Because extravascular activity is frequently very small relative to total activity in the tissue, especially for early time intervals and low values of k_1, the amount in the extravascular space is calculated as the difference between two large numbers, which may differ only in the third or fourth digit. Thus, a minor underestimation of PV, as

occurs with PBF <40, results in an extravascular curve which is much too high at early times and consequently the value for k_1 is overestimated. The exact magnitude of this overestimation will depend on the true value for k_1 and k_2 as well as the error in the calculated PV (Fig. 4).

In experimental models of lung injury, due for instance to intravenous oleic acid or to ischemia reperfusion (7,8), regional PBF values less than 70 ml/min/100 ml lung are unusual, but do occur. Very low regional PBF might also be expected in conditions of vascular destruction, such as with emphysema. The current studies suggest that as long as regional PBF is greater than 40 ml/min/100 ml, tracer concentration in the vascular compartment is independent of tracer delivery to the compartment. Thus, use of the original mathematical model (MODEL-NOPBF) should result in accurate estimates of PTCER. When regional PBF is less than 40 ml/min/100 ml lung, the estimates of PTCER may be seriously in error unless MODEL-PBF is used. However, this procedure would require either an additional parameter to be estimated (PBF) or an independent measurement of PBF to be obtained.

PV Versus Vascular Surface Area. If PV is linearly related to vascular surface area, then *changes* in PV should result in proportional changes in surface area. Assuming then that *permeability* does not in fact change, changes in PV should be accompanied by proportional changes in k_1. In the Hemorrhage group, assuming no change in true permeability, regional pulmonary PV decreased in all dogs, but k_1 decreased in only half the dogs and not proportionally to the change in PV (Fig. 2). Thus, while an accurate measurement of PV is necessary for an accurate estimate of k_1, the PV measurement itself may not be a useful means of correcting k_1 for changes in vascular surface area. A better correction for k_1 awaits a better in vivo technique for measuring vascular surface area. Fortunately, in the meantime, changes in k_1, even as a result of mild-moderate injury, appear to be very large relative to any change in surface area (7,8). Thus, the changes in k_1 (and PTCER) as a result of injury are still easily detected.

CONCLUSION

The original two-compartment mathematical model used to measure pulmonary transvascular protein flux with PET is appropriate if regional PBF is greater than approximately 40 ml/min/100 ml lung. Below this level of regional PBF, PV may be underestimated and PTCER seriously overestimated. Ideally, PTCER calculations should be accompanied by either independent measurements of regional PBF or PBF should be included in the model estimates. Even when PV is accurately measured, it may still be an inadequate measure of vascular surface area.

APPENDIX

The two models for calculating PTCER (MODEL-NOPBF, which is the model used to calculate PTCER in the experimental

protocols, and MODEL-PBF, used in the computer simulations) are described in the Methods section.

In both models, total activity at a given time ($Q(t)$) is described as:

$$Q(t) = q_1(t) + q_2(t), \qquad \text{Eq. A1}$$

where q_1 and q_2 represent the quantity of tracer (cpm) in the intravascular and extravascular compartments, respectively.

For the more complete two-compartment model (MODEL-PBF), the change in tracer activity in the intravascular and extravascular compartments is described by the following set of differential equations:

$$dq_1(t)/dt = f(Bl(t) - q_1(t)/v_1) - k_1q_1(t) + k_2q_2(t) \qquad \text{Eq. A2}$$

$$dq_2(t)/dt = k_1q_1(t) - k_2q_2(t), \qquad \text{Eq. A3}$$

where f is blood flow in units of ml/sec, Bl is the tracer concentration in the pulmonary arterial blood in cpm/100 ml, v_1 is the vascular volume in ml and k_1 and k_2 are the forward and reverse rate constants in 1/sec.

For MODEL-NOPBF, the problem is simplified by assuming that tracer concentration in the vascular space is equal to the measured pulmonary arterial blood concentration,

$$q_1(t) = v_1 (Bl(t) \qquad \text{Eq. A4}$$

since the single-pass extraction fraction of transferrin is very low. With this assumption, the tracer activity in the extravascular space is given by the following solution to Equation A3:

$$q_2(t) = k_1v_1 (Bl(t)*exp(-k_2t) \qquad \text{Eq. A5}$$

where the * denotes the convolution operation. The concentration of tracer detected by PET at any time, $C_{PET}(t)$, is given by the sum of Equations 4 and 5 divided by the pixel volume, V (ml),

$$C_{PET}(t) = [v_1Bl(t) + k_1v_1Bl(t)*exp(-k_2t)]/V. \qquad \text{Eq. A6}$$

Since only the relative vascular volume is known, the equation can be simplified for implementation by defining

$$V_1 = v_1/V \text{ and } K_1 = k_1V_1 \qquad \text{Eq. A7}$$

and substituting in Equation A6 to yield

$$C_{PET}(t) = V_1Bl(t) + K_1Bl(t)*exp(-k_2t). \qquad \text{Eq. A8}$$

To match PET scan data, $C_{PET}(t)$ is integrated over the scan intervals as described in (10).

For MODEL-PBF, the solution to differential Equations A2 and A3 can be obtained by Laplace transforms:

$$q_1(t) = [f/(e_2 - e_1)][(k_2 - e_1)exp(-e_1t)$$
$$+ (e_2 - k_2)exp(-e_2t)]*Bl(t) \qquad \text{Eq. A9}$$

$$q_2(t) = [k_1f/(e_2 - e_1)][exp(-e_1t)$$
$$- exp(-e_2t)]*Bl(t), \qquad \text{Eq. A10}$$

where the values e_1 and e_2 are roots of a quadratic equation,

$$e_1, e_2 = 1/2[a \pm \sqrt{a^2 - 4b}] \qquad \text{Eq. A11}$$

$$a = f/v_1 + k_1 + k_2, b = k_2f/v_1. \qquad \text{Eq. A12}$$

Thus, the instantaneous PET concentration is given by:

$$C_{PET}(t) = f/(V(e_2 - e_1))[(k_1 + k_2 - e_1)exp(-e_1t)$$
$$+ (e_2 - k_1 - k_2)exp(-e_2t)]*Bl(t). \qquad \text{Eq. A13}$$

To avoid the numerical computations associated with the convolution operations, the arterial blood curve is fit with a two exponential function:

$$Bl(t) = Ae^{-\alpha t} + Be^{-\beta t}. \qquad \text{Eq. A14}$$

With this approximation to the pulmonary arterial blood curve, the convolution operations shown in Equation A13 can be evaluated to yield the following equation for the instantaneous PET activity:

$$C_{PET}(t) = [DA/(e_1 - \alpha)][exp(-\alpha t)$$
$$- exp(-e_1t)] + [DB/(e_1 - \beta)][exp(-\beta t)$$
$$- exp(-e_1t)] + [EA/(e_2 - \alpha)][exp(-\alpha t)$$
$$- exp(-e_2t)] + [EB/(e_2 - \beta)][exp(-\beta t)$$
$$- exp(-e_2t)], \qquad \text{Eq. A15}$$

where the variables D and E are defined as:

$$D = (f/V)(k_1 + k_2 - e_1)/(e_2 - e_1)$$

$$E = (f/V)(e_2 - k_1 - k_2)/(e_2 - e_1). \qquad \text{Eq. A16}$$

To match the PET scan data, the integral of Equation A15 is computed in a manner analogous to that used for MODEL-NOPBF.

ACKNOWLEDGMENTS

REFERENCES

1. Gorin AB, Weidner WJ, Demling RH, Staub NC. Noninvasive measurement of pulmonary transvascular protein flux in sheep. J Appl Physiol 1978;45:225-233.
2. Gorin AB, Kohler J, DeNardo G. Noninvasive measurement of pulmonary transvascular protein flux in normal man. J Clin Invest 1980;66:869-877.
3. Dauber IM, Pluss WT, VanGrondelle A, Trow RS, Weil JV. Specificity and sensitivity of noninvasive measurement of pulmonary vascular protein leak. J Appl Physiol 1985;59:564-574.
4. Mintun MA, Dennis DR, Welch MJ, Mathias CJ, Schuster DP. Measurements of pulmonary vascular permeability with PET and gallium-68 transferrin. J Nucl Med 1987;28:1704-1716.
5. Roselli RJ, Riddle WR. Analysis of noninvasive macromolecular transport measurements in the lung. J Appl Physiol 1989;67:2343-2350.
6. Mintun MA, Warfel TE, Schuster DP. Evaluating pulmonary vascular permeability with radiolabeled proteins: an error analysis. J Appl Physiol 1990;68:1696-1706.
7. Velazquez MV, Weibel ER, Kuhn C, Schuster DP. Positron emission tomographic evaluation of pulmonary vascular permeability: a structure-function correlation. J Appl Physiol 1991;70:2206-2216.
8. Palazzo R, Hamvas A, Shuman T, Kaiser L, Cooper J, Schuster DP. Injury in nonischemic lung after unilateral pulmonary ischemia with reperfusion. J Appl Physiol 1992;72:612-620.
9. Yamamoto M, Ficke DD, Ter-Pogossian MM. Performance study of PETT VI. A positron computer tomograph with ^{248}Ce fluoride detectors. IEEE Trans Nucl Sci 1982;29:529-533.
10. Mintun MA, Ter-Pogossian MM, Green MA, Lich LL, Schuster DP.

Quantitative measurement of regional pulmonary blood flow with positron emission tomography. *J Appl Physiol* 1986;60:317–326.

11. Schuster DP, Marklin GF. The effect of regional lung injury or alveolar hypoxemia on pulmonary blood flow and lung water as measured by positron emission tomography. *Am Rev Respir Dis* 1986;133:1037–1042.

12. Moerlein SM, Welch MJ. The chemistry of gallium and indium as related to radiopharmaceutical production. *J Nucl Med* 1981;8:277–287.

13. Cooper JA, Malik AB. Pulmonary transvascular flux of transferrin. *J Appl Physiol* 1989;67:1850–1854.

14. Schuster DP, Marklin GF. Effect of changes in inflation and blood volume on regional lung density—a PET study: 2. *J Comput Asst Tomogr* 1986; 10:730–735.

SELF-STUDY TEST
Gastrointestinal Nuclear Medicine

Questions are taken from the *Nuclear Medicine Self-Study Program I*, published by The Society of Nuclear Medicine

13. insufficient period of fasting before the study
14. acute pancreatitis
15. fasting for 4 hr before the study
16. acute or chronic cholecystitis

Reasonable approaches at this point to improve the diagnostic utility of the study in Figure 1 include which of the following?

17. administer morphine sulfate, 0.04 mg/kg, intravenous, and continue imaging for an additional 30–45 min
18. continue imaging for an additional 3 hr
19. administer sincalide, 0.02 μg/kg, intravenous, administer

a second dose of ^{99m}Tc lidofenin, and image for 60 min
20. administer 200 ml of water by mouth

Which of the following characteristics among the ^{99m}Tc acetanilidoiminodiacetate (IDA) derivatives favors hepatocyte uptake and concentration in the biliary tree?

21. the structure should contain a nonpolar group
22. the structure should be lipophilic
23. high urinary excretion
24. low plasma protein binding

SELF-STUDY TEST
Gastrointestinal Nuclear Medicine
ANSWERS

ITEMS 1–5: Lactulose-H₂ Breath Testing
ANSWERS: 1, T; 2, F; 3, T; 4, T; 5, T

King and Toskes have reviewed carbohydrate-H_2 breath testing for detecting bacterial overgrowth and compared these tests with the ^{14}C-xylose breath test and intestinal culture. Although H_2 breath tests are attractive because of their ease of performance and nonradioactive nature, they are both inadequately sensitive and specific. H_2 breath tests are also affected by a number of factors that make their interpretation problematic. Cigarette smoking within 1 hr before the test elevates breath H_2; diarrhea and prior treatment with antibiotics and enemas impair bacterial production of H_2. Although earlier studies suggested that only an occasional patient may lack H_2-producing bacteria, it is now appreciated that up to 30% of patients may not generate significant H_2 with the usually employed 10-g lactulose-H_2 test; in such patients, 30 g of lactulose should be administered. It also appears that as many as 30% of patients with culture-proven bacterial overgrowth may have elevated levels of breath H_2 in the fasting state.

References

1. King CE, Toskes PP. The use of breath tests in the study of malabsorption. *Clin Gastroenterol* 1983;12:591–610.
2. King CE, Toskes PP. Comparison of the 1-gram [^{14}C]xylose, 10-gram lactulose-H_2 breath tests in patients with small intestine bacterial overgrowth. *Gastroenterology* 1986;91:1447–1451.

ITEMS 6–9: CCK Cholescintigraphy
ANSWERS: 6, F; 7, T; 8, F; 9, F

CCK cholescintigraphy should be employed to confirm a surgeon's and/or gastroenterologist's clinical impression that right upper quadrant pain and biliary colic are a manifestation of acalculous biliary disease. It should not be employed as a screening test in individuals with vague abdominal pain, because false-positive studies will occur since the maximal gallbladder ejection fraction response to CCK in this patient population has yet to be determined.

CCK cholescintigraphy can be employed as a noninvasive means of identifying patients with sphincter of Oddi dyskinesia, as some will demonstrate a CCK cholescintigraphic pattern indicative of this disorder. A delay in biliary-to-bowel transit and failure of the sphincter of Oddi to relax after CCK infusion (the dilated common duct sign) are the cardinal scintigraphic features of this dysfunctional disorder of the biliary tree.

The most accurate test for the detection of acute cholecystitis is hepatobiliary scintigraphy. Its sensitivity exceeds 95% without the use of CCK. However, pretreatment with CCK is often employed to improve the specificity of this test in patients with sludge in their gallbladders or in those who have been fasting or undergoing total parenteral feeding for prolonged periods.

False-positive CCK cholescintigrams will occur if CCK is not infused